Expert Systems With Applications 122 (2019) 102–107

Contents lists available at ScienceDirect

Expert Systems With Applications

journal homepage: www.elsevier.com/locate/eswa

Automatic object detection using dynamic time warping on ground penetrating radar signals

Sajad Jazayeri[a], Abolfazl Saghafi[b,*], Sanaz Esmaeili[a], Chris P. Tsokos[c]

[a] School of Geosciences, University of South Florida, Tampa, FL, USA
[b] Department of Mathematics, Physics and Statistics, University of the Sciences, Philadelphia, PA, USA
[c] Department of Mathematics and Statistics, University of South Florida, Tampa, FL, USA

ARTICLE INFO

Article history:
Received 14 April 2018
Revised 23 October 2018
Accepted 30 December 2018
Available online 31 December 2018

Keywords:
Ground Penetrating Radar signals
Dynamic Time Warping
Sequential confidence intervals
Control process
Object detection

ABSTRACT

Ground Penetrating Radar (GPR) is a widely used non-destructive method in buried object detection. However, online, automatic, and accurate location and depth estimation methods using GPR are still under development. In this article, a cutting-edge expert system is proposed that compares signals from newly scanned locations to a target-free accumulated reference signal and computes a dissimilarity measure using Dynamic Time Warping (DTW). By setting a threshold on DTW values and monitoring them online, a significant deviation of the DTW values from the reference signal is detected prior to reaching an object. A potential burial site is therefore automatically detected without having a complete GPR scan which is a huge advantage compared to existing methods. Following the scanning process and investigating the potential burial site, location and depth of multiple buried objects is estimated automatically and highly accurate. The fully-automated analytics eliminate the need of expert operators in estimating spatial burial locations and perform accurately even on noisy media. Statistical proofs are provided that support the validity of the developed expert system in theory. Moreover, the analytics run in real-time that is plausible for on-site applications.

1. Introduction

Ground Penetrating Radar (GPR) is widely used in detecting buried objects including utility lines, tree roots, caves, landmines, grave sites, etc. (Daniels, 2005). GPR transmits high frequency electromagnetic waves which can pass through soil and possibly underground objects. A portion of the wave is reflected after hitting anomalies with different electromagnetic properties from that of surrounding soil and is received by an antenna. The signature of buried objects in a reflected GPR signal is likely to be hyperbolic shaped (Benedetto & Pajewski, 2015; Pettinelli et al., 2009; Zeng & Mc Mechan, 1997). Further analysis of the reflected signals leads to buried object detection, location and depth estimation.

Accurate depth estimation of the lateral object location depends on two factors: the user's judgment to peak the apex of the diffraction hyperbola and good velocity approximation of the wave in the media. Biassed depth estimation commonly happens by operator's errors while making decision about the first arrival time of the hyperbola apex and fitting the hyperbola to estimate the velocity (Jazayeri, Klotzsche, & Kruse, 2018; Sham & Lai, 2016). Indeed, decision making for noisy data or data collected over disturbed media is more challenging. Inexperienced users can interpret the data incorrectly and make inaccurate decisions. Moreover, multiple buried objects complicate the estimation process especially when objects are relatively close. In real-world problems, some objects produce very weak diffracted signals, making the signals more challenging to interpret. Thus, the importance of this topic led us to establish an automatic method to accurately calculate the location and depth of multiple buried targets.

With the widespread use of machine learning algorithms to automate object detection process, there has been some improvements in this area. For instance, utility and object detection using neural networks and pattern recognition methods (Al-Nuaimy et al., 2000; Birkenfeld, 2010; Maas & Schmalzl, 2013). While Al-Nuaimy et al. (2000) proposed a sophisticated near real-time multi-stage process to accurately identify the depth and position of buried targets, its execution however, is not fully-automated and performance depends on the quality of GPR images. Birkenfeld (2010) and Maas and Schmalzl (2013) proposed a process to only detect presence of buried objects with high accuracy. Their method, like other neural network systems, requires training examples in similar environments and performance depends

* Corresponding author.
E-mail addresses: sjazayeri@mail.usf.edu (S. Jazayeri), a.saghafi@usciences.edu (A. Saghafi), esmaeili@mail.usf.edu (S. Esmaeili), ctsokos@usf.edu (C.P. Tsokos).

https://doi.org/10.1016/j.eswa.2018.12.057
0957-4174/

on the neural network structure. Moreover, these techniques fail in presence of incomplete or highly disturbed profiles.

Other machine learning driven approaches include utilizing Genetic Algorithm (GA) with Support Vector Machine (SVM) classifier for object detection and material recognition with 80% accuracy (Pasolli, Melgani, Donelli, Attoui, & De Vos, 2008). Automatic detection and material classification of buried objects with 92% accuracy using Support Vector Machine (SVM) after applying discrete wavelet transform (DWT) and fractional Fourier transform (FRFT) (Lu, Pu, & Liu, 2014). While accuracy of theses systems is relatively high and their material recognition task is impressive, theses systems are not fully automatic and do not provide a depth estimation which is of utmost importance in real applications.

Alternative approaches include utilization of signal processing techniques such as wavelet and Hough transform to approximate the top of the hyperbola (Li et al., 2016; Qiao, Qin, Ren, & Wang, 2015). Qiao et al. (2015) proposed a multi-stage process called the Multiresolution Monogenic Signal Analysis (MMSA) which detected targets and estimated their horizontal and vertical position with average 5.8 cm distance error. Their system shows premising performance but is passive and requires expert operators. Li et al. (2016) developed a system utilizing randomized Hough transform to detect tree roots with approximately 80% accuracy and a false alarm rate of less than 1.5 m. Their method performs quite well in detecting clustered pattern of woody cellular material with weaker reflection signal but it does not provide depth estimation and no comment is made on the running time of the process.

Most recently, a thresholding method is presented by Dou, Wei, Magee, and Cohn (2017) that utilizes a column-connection clustering to separate regions of interest from background when sharp and strong reflected signals are recorded. The method utilizes an orthogonal-distance hyperbola fitting which performs reliably even with distorted or incomplete hyperbolic signatures. The system's performance is provided only in terms of average detection rate, F-measure of 0.702, and no location/depth estimation performance measure was provided for comparison.

In this article, a novel automatic object detection analytic is proposed that monitors the GPR signals for potential burial sites. The monitoring step reduces the computation time significantly. Following discovery of a potential burial site, a throughout investigation of neighboring locations is conducted. The location and the depth of the object is then estimated after automatically approximating the velocity of the media. The method is applied to numerous synthetic models and a real-life multiple object situation with splendid results.

The fully-automated decision-making process proposed in this article eliminates the need of expert operators. Most importantly, a warning is issued by the expert system when approaching a potential burial site that provides a significant military application to detect explosives ahead. Further, the spatial burial location of multiple objects is accurately estimated even on challenging noisy media.

2. Materials

Three scenarios are considered to generate synthetic data, 20 cases of each were generated to evaluate accuracy of the proposed method. Scenario 1 with no buried object but noisy data. Scenario 2 where a cylindrical PVC pipe with a wall thickness of 3 mm and inner diameter of 10 cm is buried in sand, in a random location, at a random depth. No noise has been added to the data in this scenario. Pipes are considered to be water-filled, like most liquid-filled utility pipes. Scenario 3 in which additive noise is added to the data from Scenario 2 to imitate a more realistic situation. The additive noise is assumed to be a combination of white noise with Gaussian distribution, signal to noise ratio of 25 dB, and random outliers (Jazayeri, Ebrahimi, & Kruse, 2017). The synthetic models are created in two dimensions using the FDTD gprMax code (Warren, Giannopoulos, & Giannakis, 2016). In the simulated cases, materials considered to be homogeneous (see Table 1). The transmitted wavelet is a ricker waveform with the central frequency of 800 MHz. The antenna offset is 14 cm and the trace interval is set to 2.5 cm.

Table 1
Material properties.

Media	Relative permittivity	Electrical conductivity (mS/m)
Soil	5	1
PVC pipe	3	1
Water	80	1

Aside from synthetic models, a real case is considered where data collected on a main road covered with asphalt with pipes and drainage channels underneath at unknown locations and depths. The data is collected with a 800 MHz shielded antenna MALA ProEx system. A small portion of a GPR profile is used in this article which includes a pipe and a drainage channel.

3. Methods

DTW algorithms align two signals in time dimension by creating a so-called "warping path" and determining a measure of their dissimilarity independent of certain non-linear variations (Ratanamahatana & Keogh, 2004). This alignment method provides a powerful tool in signal classification, aiming to group similar signals based on their distance, and has numerous applications in automated decision making (Berndt & Clifford, 1994; Cao, Rakhilin, Gordon, Shen, & Kan, 2016; Kaczmarek & Staworko, 2009).

Given two signals $A = (a_1, \ldots, a_n)$ and $B = (b_1, \ldots, b_m)$ not necessarily with equal length, the DTW process starts by constructing an $n \times m$ matrix in which the element of the (i, j)th component corresponds to the following squared Euclidian distance

$$d\left(a_i, b_j\right) = \left(a_i - b_j\right)^2. \tag{1}$$

The process then continues by retrieving a path through the matrix that minimizes the total cumulative distance between the two signals as illustrated in Fig. 1. Specifically, the optimal path is found by minimizing the warping cost given by

$$DTW(A, B) = \sqrt{\sum_{k=1}^{K} d_k}, \tag{2}$$

where d_k is the kth element of the warping path. The optimal path is found using an iterative method. The proposed general procedure to detect hidden buried objects using DTW is as follows:

(a) Three target-free locations are scanned with GPR and the average of their signals is considered as the reference signal for the current under investigation ground.
(b) Proceed by scanning target areas and computing the DTW distance of the new locations with the reference signal. The more similar the signals are to the reference signal, the smaller their distance value. Setting a threshold on the computed sequential dissimilarity measures assists in detecting potential burial sites.
(c) The DTW values increase gradually by getting closer to a site with buried objects. Finding a site where a local peak of DTW happens and investigating the surrounding locations to trace a hyperbola will lead to a highly probable burial location.

Graph of the computed dissimilarity measures for case #7 in the three discussed scenarios along with the profiles is shown in

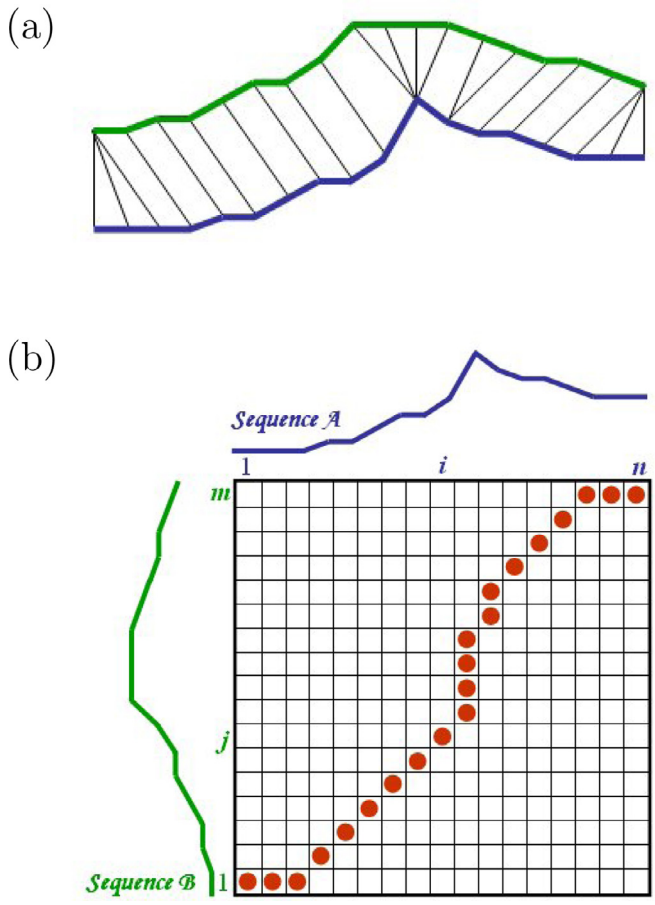

Fig. 1. (a) A non-linear Dynamic Time Warp and (b) warping path between two signals of equal length.

Fig. 2. Obviously, target-free locations have similar signals to the reference signal since their DTW value randomly fluctuates. Getting closer to the buried object results in higher signal dissimilarity and higher DTW value in the 2nd and 3rd scenarios. The increasing pattern in DTW values are detectable even in noisy environment of the 3rd scenario.

In the next section, a statistical approach is developed to detect buried objects when approaching them while keeping the detection failure error controlled. The procedure is an online sequential control process that monitors GPR signals as they are recorded and is capable of detecting multiple objects.

4. Theory/calculations

Suppose $\boldsymbol{x}_n = \left(x_n^1, x_n^2, \ldots, x_n^T\right)$ is the nth recorded GPR signal with T as the signal length; $\boldsymbol{x}_1$, $\boldsymbol{x}_2$, and $\boldsymbol{x}_3$ are recorded from target-free locations and their average serves as the reference signal. Let d_n be the DTW distance of the nth recorded signal and the reference signal computed using (2). Let $\bar{d}_n^4$ represent the window average of the last 4 DTW values given by

$$\bar{d}_n^4 = \frac{1}{4}\sum_{i=n-3}^{n} d_i, \tag{3}$$

and $\bar{d}_n^{25}$ represent the window average of the last 25 DTW values given by

$$\bar{d}_n^{25} = \frac{1}{25}\sum_{i=n-24}^{n} d_i, \tag{4}$$

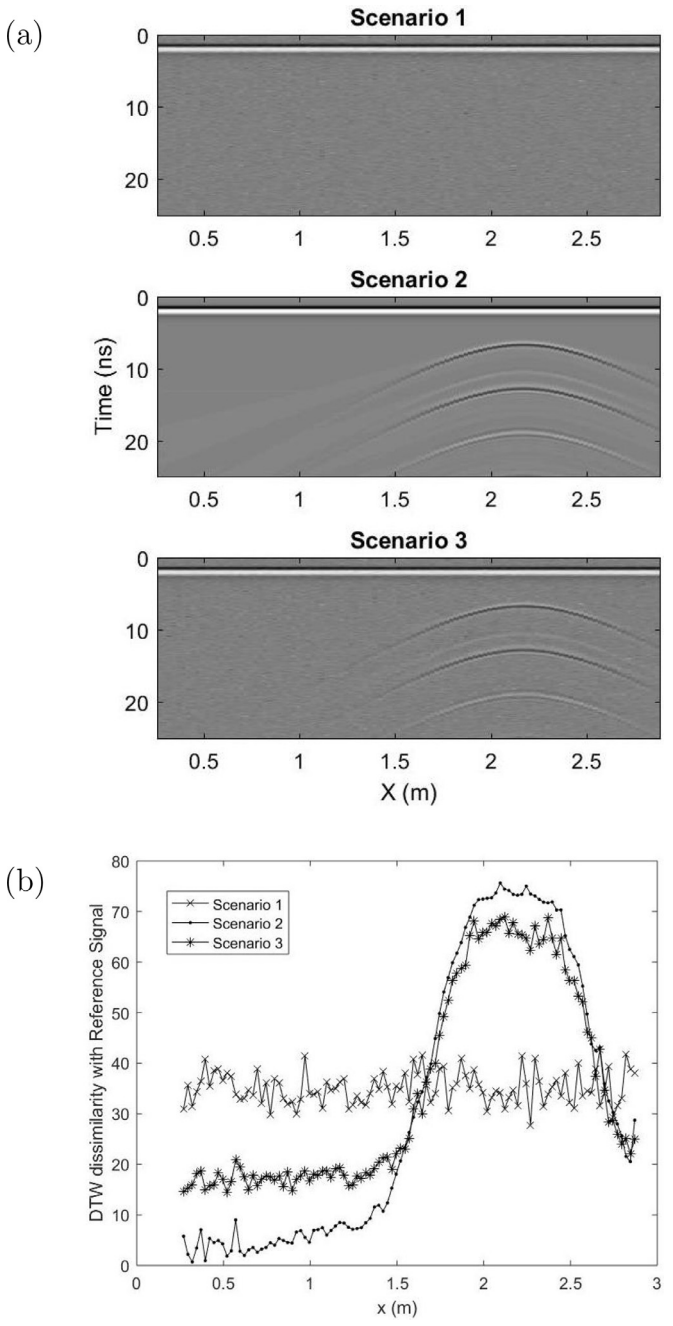

Fig. 2. (a) GPR profiles and (b) DTW dissimilarity measures from reference signal for case #7 in the three experimental scenarios.

where the window average of 25 is computed for the available values at the beginning of the process and is shown by $\bar{d}_n^n$.

Lemma 1. *As soon as the nth signal is recorded, the following decision boundary detects underground objects with probability 0.999 for* $n \geq 25$*:*

$$\bar{d}_n^4 > \bar{d}_n^{25} + u_n^{25}, \tag{5}$$

where

$$u_n^{25} = t_{(24,0.999)} s_n^{25}\left(\frac{21}{25^2}\right)\left(1 + \frac{21}{4^2}\right). \tag{6}$$

For $4 \leq n \leq 24$*, the following boundary detects underground objects with the same probability:*

$$\bar{d}_n^4 > \bar{d}_n^n + u_n^n, \tag{7}$$

Table 2
Mean Absolute Error (cm) and Root Mean Square Error (cm) of the DTW analytics in 20 simulated cases for two scenarios.

Scenario	Location			Depth	
	Detection	MAE	RMSE	MAE	RMSE
Scenario 2	104.85	0.474	0.725	1.872	2.351
Scenario 3	104.35	0.600	1.432	2.258	2.723

where

$$u_n^n = t_{(n-1,0.999)} s_n^n \left(\frac{n-4}{n^2}\right)\left(1+\frac{n-4}{n^2}\right). \quad (8)$$

The proof of the lemma is provided in the appendix. The computational steps to utilize the lemma are as follows:

1. When $\boldsymbol{x}_n (n \geq 4)$ is recorded and the surface reflection is removed, its DTW distance from the reference signal is computed along with the window average of four $\left(\bar{d}_n^4\right)$ and the window average of 25 ($\bar{d}_n^{25}$ or $\bar{d}_n^n$ when applicable).
2. A one-sided t-student confidence interval $(0,\ \bar{d}_n^{25} + u_n^{25})$ is generated using (6). When there are less than 25 observations this interval is size dependent and is computed as $(0,\ \bar{d}_n^n + u_n^n)$ using (8).
3. If $\bar{d}_n^4 \leq \bar{d}_n^{25} + u_n^{25}$ (or $\bar{d}_n^4 \leq \bar{d}_n^n + u_n^n$ when applicable) then process is under control and the chance of failure in detection is $\alpha = 0.001$. Otherwise, a warning is generated and an object underground is detected ahead. In this case, values of $\bar{d}^4$ keeps increasing by approaching the buried object.
4. Scanning target areas and monitoring continues until a local peak of $\bar{d}^4$ is observed. This peak happens in the vicinity of a highly probable burial site, $\boldsymbol{x}_n (a \leq n \leq b)$.
5. A hyperbola is tracked and mapped for signals of the probable burial site through analytic searching. The location of the buried object is estimated as the apex of the hyperbola curve.
6. A least-square approach is used to approximate the velocity using the marked nodes on the diffracted hyperbola in step 5. Then, the one-way travel time of the wave at the estimated location of the target is multiplied by the velocity to estimate the depth. A zero-time correction is applied beforehand where the zero-time is estimated using the potential burial site signals.
7. The process is repeated for all the local peaks of $\bar{d}^4$ for detecting multiple objects.

5. Results

The results of the proposed decision analytics for case #7 in the three discussed scenarios is illustrated in Fig. 3. Due to limited space, it is not possible to include all cases, however all the results are available as supplementary materials. In the 1st Scenario where there was nothing underground, the confidence limit randomly fluctuates with no increasing pattern. There are some values outside the confidence limit but that does not change the pattern of the upper interval. In the 2nd Scenario however, the confidence limit increases due to severe dissimilarity of the new signals from the reference signal. A warning message generated at $x = 0.995$ m and the burial location estimated as $x = 2.17$ m. The burial depth is approximated as 0.3497 m underground. The true location of the object was 2.17 m, 0.350 m underground, i.e. <0.08% error in depth estimation and exact predicted location. In the 3rd Scenario, an increasing pattern for the confidence bound is observed as well. A warning is issued at $x = 1.37$, the buried object estimated to be at $x = 2.17$, 0.363 m underground; ~3.7% error in depth due to additive noise and random outliers.

The performance of the proposed method in 20 simulated experiments of Scenarios 2 and 3 is presented in Table 2. All 20 cases

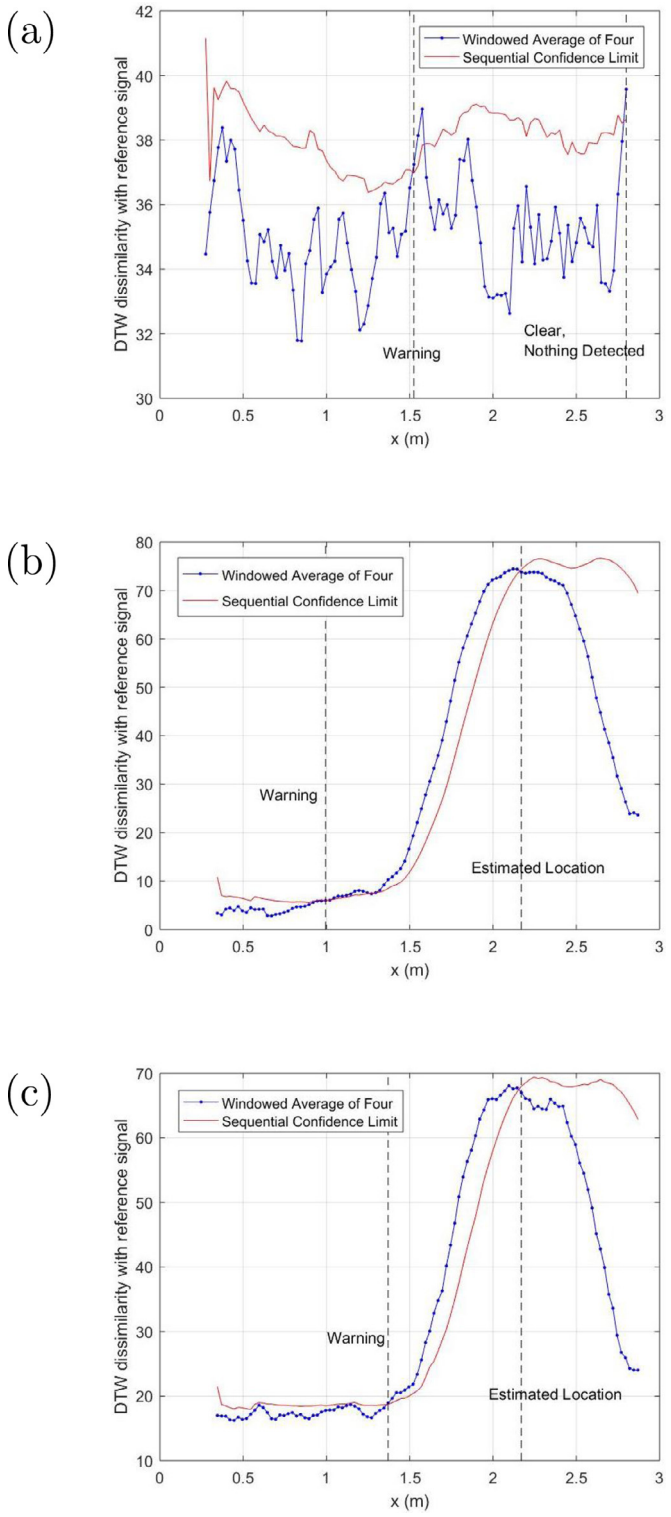

Fig. 3. DTW dissimilarity measure and sequential confidence intervals for case #7 in the three experimental scenarios, (a) Scenario 1, (b) Scenario 2, (c) Scenario 3.

in 1st scenario were successfully marked "clear site" using the proposed approach, while all the cases in Scenario 2 and 3 warned for a burial site. On average, the warning message was generated 1.05 m prior to reaching the object in the 2nd scenario. The Mean Absolute Error (MAE) and Root Mean Squared Error (RMSE) of the location estimation for the 2nd scenario was 0.47 and 0.73 cm, respectively; meaning that on average the locations were estimated

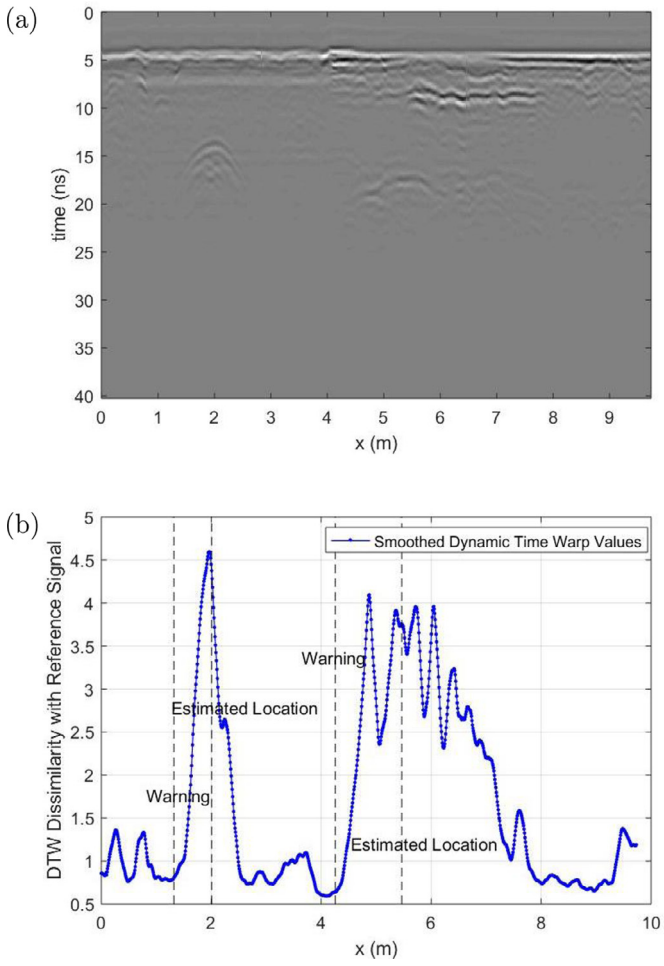

Fig. 4. (a) A real GPR experimental profile (b) DTW warning and estimated locations.

with 0.47 cm error; RMSE reflects both bias and variation in estimations. The depth estimation was accurate as well, with 1.872 and 2.351 cm for MAE and RMSE, respectively. For cases in the 3rd scenario, on average the proposed analytics could detect a buried object from 1.04 m away. The MAE and RMSE in these scenarios were 0.60 and 1.43 cm for location; 2.26 and 2.72 for depth estimation, respectively.

The outcome of DTW approach on the real case scenario is illustrated in Fig. 4. As the GPR profile shows, there are random noises and distortions in the GPR signal that scramble the signal in many locations, making it difficult for many methods to perform adequately. However, the DTW process performs exemplary by estimating the location of multiple objects as $x = 2.007$ and $x = 5.447$, respectively 0.541 and 0.779 m underground. The exact locations and depths in this real experiment are unknown but the results match expert expectations. The complex reflection surrounding the second object may be created by a combination of two closely-spaced utilities; the sharp local peak of the DTW plot at 4.9 m may be created by the first following by the second and wider object (drainage channel) which is detected by the analytics as a definite target. Here, the analytics pick on the local max of the smoothed DTW values happening at 4.90 and track the trace of the hyperbola using a custom window search to reach its peak.

The method proposed in this paper, presented complete success in detecting the subsurface anomalies in all studied cases of synthetic and real data. To our experience, even the most recent detection method proposed by Dou et al. (2017), fails to locate the drainage channel at 5 m in Fig. 4(a) while the proposed method successfully detects the object and performs valid depth estimation using imperfect hyperbolic signatures. Moreover, the presented statistical measures of estimation accuracy provide a reliable comparison tool for alternate approaches.

6. Conclusions and discussion

In this article, a statistical monitoring scheme is introduced that measures dissimilarity of GPR signals to signals from target-free locations to automatically detect multiple hidden buried objects and estimate their location as well as depth. The computations are performed in real-time. All the synthetic and real data used to generate the results are accessible via the corresponding authors' personal webpage.[1] Statistical proof provided in the appendix validates the effectiveness of the proposed analytics.

An alarm is generated to warn the user when a potential burial site is detected ahead by setting a threshold on the values of the dissimilarity measure. This provides a huge advantage over alternate techniques which require full GPR information to detect burial sites. The threshold was set using a t-student distribution. Sensitivity of the alarm generation could be controlled by changing the critical value α, default value is set to 0.001.

Although we used the average of three target-free locations as the reference signal, more samples could be used to generate the reference; less than two is not recommended. In addition, we have utilized an average window of four DTW's for checking in/out of control states since four samples cut the length of the interval in half. A window average of 25 DTW's has been utilized to create confidence limits using t-distribution following Central Limit Theorem. Investigations could be made to determine probable more suitable window sizes.

The proposed system is not entirely flawless and can be improved. Different settings in synthetic and real-life situations on hyperbola mapping are used to achieve accurate results. This suggests possibly new settings for different GPR devices for reliable implementation. Moreover, the depth estimation in the proposed system depends on the soil velocity approximation. A custom hyperbola search and mapping is used in the analytics to approximate velocity by computing signal's travel time. While this approach performed well on all our synthetic and real-life data, it still could be improved. Looking into alternate techniques to approximate soil velocity and an even better hyperbola mapping technique is a possible future development.

A prominent future research is accurately pinpointing spatial location of objects that are buried in close proximity, e.g. in detecting reinforcement steel bars. In this case, the hyperbolas intervene which make their mapping challenging. However, one can use pooled information from multiple objects buried at the same depth to make an even more reliable depth estimation. Furthermore, our analytics require full GPR profile to make a reliable depth estimation. One potential future development is to use the symmetry of hyperbola and mathematical modeling to reduce the amount of information required for depth estimation. In addition, an expert 2D decision-making process could be developed that utilizes the proposed analytics to search an area for potential buried objects while creating a 2D map of the DWT values. Eventually the searching process could be automatized completely with a proper decision circuit.

Acknowledgments

The authors are grateful to Dr. Sarah Kruse and anonymous reviewers for their constructive comments.

[1] AbolfazlSaghafi.info/research.

Appendix A. Proof of Lemma 1

The proof is provided for $n \geq 25$ while steps are similar for $4 \leq n \leq 24$. Under the hypothesis that there is nothing underground, the window average of 25 and 4 have the same expected value, that is:

$$E\left(\bar{D}_n^4\right) = \mu^4 = \mu^{25} = E\left(\bar{D}_n^{25}\right),$$

where μ^4 is the true mean of the window average of 4 DTW distance values and μ^{25} is the true mean of the window average of 25 DTW distance values. However, by approaching target-locations, the window average of 4 increases promptly while the window average of 25 increases gradually. To detect this change as quickly as possible, we are testing the following statistical hypothesis at each step of the process:

$$H_0 : \mu^4 = \mu^{25} \qquad Vs \qquad H_1 : \mu^4 > \mu^{25},$$

The test statistic is $(\bar{D}_n^4 - \bar{D}_n^{25})$, which is unbiased under null-hypothesis:

$$E\left(\bar{D}_n^4 - \bar{D}_n^{25}\right) = 0,$$

and has the following variance

$$Var\left(\bar{D}_n^4 - \bar{D}_n^{25}\right) = \sigma^2\left(\frac{21}{25^2}\right)\left(1 + \frac{21}{4^2}\right),$$

where $Var\left(\bar{D}_n^n\right) = \sigma^2/n$. Thus, using Central Limit Theorem, one concludes

$$\frac{\left(\bar{D}_n^4 - \bar{D}_n^{25}\right)}{\sigma^2\left(\frac{21}{25^2}\right)\left(1 + \frac{21}{4^2}\right)} \approx N(0, 1).$$

By estimating σ^2 using the last 25 observations, we have

$$\frac{\left(\bar{D}_n^4 - \bar{D}_n^{25}\right)}{s_n^{25}\left(\frac{21}{25^2}\right)\left(1 + \frac{21}{4^2}\right)} \approx t_{(24)},$$

where

$$s_n^{25} = \sqrt{\frac{1}{24}\sum_{i=n-24}^{n}\left(D_i - \bar{D}_n^{25}\right)^2}.$$

Thus, an α-level rejection region for testing H_0 against H_1 will be

$$\left(\bar{D}_n^4 - \bar{D}_n^{25}\right) > t_{(24,\ \alpha)}s_n^{25}\left(\frac{21}{25^2}\right)\left(1 + \frac{21}{4^2}\right).$$

Therefore, using a t-distribution confidence interval, a buried object is detected when $\left(\bar{d}_n^4 - \bar{d}_n^{25}\right) > u_n^{25}$, where

$$u_n^{25} = t_{(24,\alpha)}s_n^{25}\left(\frac{21}{25^2}\right)\left(1 + \frac{21}{4^2}\right),$$

As long as $\left(\bar{d}_n^4 - \bar{d}_n^{25}\right) \leq u_n^{25}$, the process is under control and the probability of not detecting a change equals α which is related to the selected t-distribution critical value and controls the sensitivity of the test.

Supplementary material

Supplementary material associated with this article can be found, in the online version, at doi:10.1016/j.eswa.2018.12.057.

References

Al-Nuaimy, W., Huang, Y., Nakhkash, M., Fang, M., Nguyen, V., & Eriksen, A. (2000). Automatic detection of buried utilities and solid objects with GPR using neural networks and pattern recognition. *Journal of applied Geophysics, 43*(2), 157–165.

Benedetto, A., & Pajewski, L. (2015). *Civil engineering applications of ground penetrating radar*. Springer.

Berndt, D. J., & Clifford, J. (1994). Using dynamic time warping to find patterns in time series. In *Proceedings of the 3rd international conference on knowledge discovery and data mining: 10* (pp. 359–370). WA: Seattle.

Birkenfeld, S. (2010). Automatic detection of reflxion hyperbolas in GPR data with neural networks. In *IEEE world automation congress (WAC)* (pp. 1–6). Japan: Kobe.

Cao, Y., Rakhilin, N., Gordon, P. H., Shen, X., & Kan, E. C. (2016). A real-time spike classifiation method based on dynamic time warping for extracellular enteric neural recording with large waveform variability. *Journal of neuroscience methods, 261*, 97–109.

Daniels, D. J. (2005). Ground penetrating radar. *Wiley Online Library*.

Dou, Q., Wei, L., Magee, D. R., & Cohn, A. G. (2017). Real-time hyperbola recognition and fitting in GPR data. *IEEE Transactions on Geoscience and Remote Sensing, 55*(1), 51–62.

Jazayeri, S., Ebrahimi, A., & Kruse, S. (2017). Sparse blind deconvolution of common-offset GPR data. In *SEG technical program expanded abstracts* (pp. 5140–5145). Society of Exploration Geophysicists.

Jazayeri, S., Klotzsche, A., & Kruse, S. (2018). Improving estimates of buried pipe diameter and infilling material from ground-penetrating radar profiles with full-waveform inversion. *Geophysics, 83*(4), H27–H41.

Kaczmarek, A., & Staworko, M. (2009). Application of dynamic time warping and cepstrograms to text-dependent speaker verification. In *Proceedings of IEEE signal processing algorithms, architectures, arrangements, and applications* (pp. 169–174). Poland: Poznan.

Li, W., Cui, X., Guo, L., Chen, J., Chen, X., & Cao, X. (2016). Tree root automatic recognition in ground penetrating radar profiles based on randomized hough transform. *Remote Sensing, 8*(5), 430.

Lu, Q., Pu, J., & Liu, Z. (2014). Feature extraction and automatic material classification of underground objects from ground penetrating radar data. *Journal of Electrical and Computer Engineering, 2014*, 28.

Maas, C., & Schmalzl, J. (2013). Using pattern recognition to automatically localize reflection hyperbolas in data from ground penetrating radar. *Computers & Geosciences, 58*, 116–125.

Pasolli, E., Melgani, F., Donelli, M., Attoui, R., & De Vos, M. (2008). Automatic detection and classification of buried objects in GPR images using genetic algorithms and support vector machines. In *IEEE international geoscience and remote sensing symposium, IGARSS 2008, Boston, MA* (pp. 525–528).

Pettinelli, E., Di Matteo, A., Mattei, E., Crocco, L., Soldovieri, F., Redman, J. D., et al. (2009). GPR response from buried pipes: Measurement on field site and tomographic reconstructions. *IEEE Transactions on Geoscience and Remote Sensing, 47*(8), 2639–2645.

Qiao, L., Qin, Y., Ren, X., & Wang, Q. (2015). Identification of buried objects in GPR using amplitude modulated signals extracted from multiresolution monogenic signal analysis. *Sensors, 15*(12), 30340–30350.

Ratanamahatana, C. A., & Keogh, E. (2004). Everything you know about dynamic time warping is wrong. In *Third workshop on mining temporal and sequential data* (pp. 22–25). Citeseer.

Sham, J. F., & Lai, W. W. (2016). Development of a new algorithm for accurate estimation of GPRs wave propagation velocity by common-offset survey method. *NDT & E International, 83*, 104–113.

Warren, C., Giannopoulos, A., & Giannakis, I. (2016). gprMax open source software to simulate electromagnetic wave propagation for ground penetrating radar. *Computer Physics Communications, 209*, 163–170.

Zeng, X., & Mc Mechan, G. A. (1997). GPR characterization of buried tanks and pipes. *Geophysics, 62*(3), 797–806.